

NATIONAL INSTITUTE FOR FUSION SCIENCE

Recommended Data on Proton-Ion Collision Rate Coefficients  
for Fe XVII - Fe XXIII Ions

I. Skobelev, I. Murakami and T. Kato

(Received - Dec. 21, 2006 )

NIFS-DATA-99

Jan. 2007

RESEARCH REPORT  
NIFS-DATA Series

This report was prepared as a preprint of work performed as a collaboration research of the National Institute for Fusion Science (NIFS) of Japan. The views presented here are solely those of the authors. This document is intended for information only and may be published in a journal after some rearrangement of its contents in the future.

Inquiries about copyright should be addressed to the Research Information Office, National Institute for Fusion Science, Oroshi-cho, Toki-shi, Gifu-ken 509-5292 Japan.

E-mail: [bunken@nifs.ac.jp](mailto:bunken@nifs.ac.jp)

**<Notice about photocopying>**

In order to photocopy any work from this publication, you or your organization must obtain permission from the following organization which has been delegated for copyright clearance by the copyright owner of this publication.

Except in the USA

Japan Academic Association for Copyright Clearance (JAACC)

6-41 Akasaka 9-chome, Minato-ku, Tokyo 107-0052 Japan

Phone: 81-3-3475-5618 FAX: 81-3-3475-5619 E-mail: [jaacc@mtd.biglobe.ne.jp](mailto:jaacc@mtd.biglobe.ne.jp)

In the USA

Copyright Clearance Center, Inc.

222 Rosewood Drive, Danvers, MA 01923 USA

Phone: 1-978-750-8400 FAX: 1-978-646-8600

**RECOMMENDED DATA ON PROTON-ION COLLISION RATE COEFFICIENTS  
FOR FE XVII – FE XXIII IONS.**

**Skobelev, I.<sup>(1)(2)(3)</sup>, Murakami, I.<sup>(1)</sup>, Kato, T.<sup>(1)</sup>**

*(1) National Institute for Fusion Science, Oroshi-cho, Toki, Gifu, 509-5292, Japan*

*(2) Multicharged Ions Spectra Data Center of VNIIFTRI, Mendeleevo, Moscow region,  
141570 Russia*

*(3) Associated Institute for High Temperatures Russian Academy of Sciences, Izhorskaya  
13/19, Moscow, 125412 Russia*

**Abstract.**

Proton-ion collisions are important for excitation or de-excitation of some ion levels in a high-temperature plasma. In this present work evaluation of data obtained for proton-induced transitions in Fe XVII – Fe XXIII ions with the help of different theoretical methods is carried out. To express the evaluated data, it is used a simple analytical formula with 7 parameters, allowing to describe dependency of proton rate coefficient as a function of proton temperature in a wide temperature range. The values of free parameters have been determined by fitting of an analytical formula to numerical data and are presented as recommended data together with fitting accuracies. The obtained results can be used for plasma kinetic calculations and for development of spectroscopy methods of plasma diagnostics.

**Keywords:** ion-ion collisions, excitation, plasma spectroscopy, ion kinetics.

## 1. Introduction

The importance of proton-ion collisions for ion kinetic calculations was first demonstrated by Seaton [1] for the case of Fe XIV ion. It has been shown that the proton excitation rates can become comparable (or even larger) to the electron excitation rates for transitions for which the excitation energy  $\Delta E$  is much smaller than the proton temperature  $kT_p$ . It should be noted that in many cases proton-ion collisions are not important for formation of population of ion levels even in the case  $\Delta E \ll kT_p$ , i.e. this condition is necessary but not enough, because of the competition with electron collisions. Proton collisions can influence on the population kinetics by increasing either excitation rates for some levels or their collision decay rates.

Excitation by proton impact can be important only for levels  $i$  placed close to the ion ground state (or close to the metastable state). In this case the proton collision may be necessary to be taken into account for plasma with low electron density,  $N_e$ , otherwise electron collisions dominate the level population. Namely, the electron density  $N_e$  needs to satisfy the condition

$$N_e < A_i / C_i^e, \quad (1)$$

where  $A_i$  and  $C_i^e$  are the probability of radiative and electron collision decay of  $i$  level, respectively. At higher density electron collision is dominant and causes Boltzmann population of  $i$ -level.

Deexcitation by proton impact can be important for excited levels  $i$  if proton density satisfy the reverse condition

$$N_p > A_i / C_i^p. \quad (2)$$

If radiative decay of level  $i$  is an allowed transition, this condition can be valid only in the dense plasma (laser-produced plasma, Z-pinch, exploding wires), while for metastable levels it can be satisfied even in low dense astrophysical or laboratory plasma.

Thus, proton excitation/de-excitation of fine-structure transitions involving ground or low-lying ion metastable states is of our primary interest.

At present time there are a lot of papers where proton-ion collision rates  $C_{ij}$  have been calculated for different Fe ions. In these papers proton collision rate coefficients were published in a table form. For many applications table form of data presentation is not very convenient, and some analytical expressions for  $C_{ij}(T_p)$  would be preferable. In the present work we have used a simple function suggested in our previous paper [2] to approximate calculated temperature dependencies of  $C_{ij}(T_p)$ :

$$C_{ij}(T_p)[cm^3s^{-1}] = 10^{-10} p_1 \exp(-(p_2/T_p)^{p_3}) \frac{(T_p/p_6)^{p_7}}{1 + (T_p/p_4)^{p_5}} \quad (3)$$

This function (3) contains 7 free parameters and allows describing numerical data with accuracy better than 5% for all transitions in all ions considered. The values of free parameters are presented in Table 1 together with approximation accuracies.

Several semiclassical methods can be employed in deriving proton rate coefficients (see, for example, reviews [3-6]). The semiclassical (or impact-parameter) approach in which the position of the proton relative to the ion is treated classically was originally applied to Coulomb excitation of nuclei by Alder *et al.* [7] and first extended to the proton excitation of ions by Seaton [1]. In the case of semiclassical calculations, either first-order approximations or close-coupling approximations have been used.

At low proton energies semiclassical first-order approximation is valid at all impact parameters because the interactions between proton and electrons of ion are weak due to Coulomb repulsion of proton and ion. At intermediate energies and low impact parameter values the first-order approximation fails, and it is necessary to adopt a different approximation or to solve the coupled differential equations describing the interaction numerically. In the semiclassical close-coupling approximation, the transition probabilities are determined by means of the numerical solution of coupled differential equations, thereby removing the need for first-order approximations and hence the uncertainty in the intermediate energy range.

Generally speaking, the most accurate method is to treat the proton's trajectory quantum mechanically and solve the complete set of close-coupling equations. Such an approach is commonly used in R-matrix calculations of electron-ion collisions; however, it is computationally much more demanding for proton collisions and practically no results were obtained for Fe XVII-XXIII ions by this method. Within the semiclassical approach, it has been shown that symmetrizing the problem with respect to the initial and final velocities (Alder *et al.* [7]), and including polarization effects (Heil *et al.* [8, 9]), can improve the accuracy of the proton rates. In paper of Faucher & Landman [10] it has been shown that for highly charged ions quantum approach and semiclassical close-coupling one can give very close results.

## 2. Results

### Ne-like Fe ion ( $2s^2 2p^5 3s \ ^3,^1P_J - \ ^3,^1P_J$ ).

For Ne-like Fe ions (Fe XVII) we know only one paper of Landman [11] where

proton collisional excitation rate coefficients were calculated for transitions among the  $2p^53s$   $^3P_0$ ,  $^3P_1$ ,  $^3P_2$ , and  $^1P_1$  levels. The calculations were performed according to symmetrized semiclassical impact parameter theory in which the truncated Schroedinger equation for quadrupole excitation was integrated directly. Intermediate coupling wave functions for the  $J = 1$  levels were determined using the observed  $2p^53s$  energy levels; for others, the Slater and spin-orbit interaction integrals obtained with Froese Fischer's MCHF77 program [12] were used. The LS-coupled quadrupole interaction matrix was then converted to intermediate coupling according to the derived transformation coefficients.

The results of Landman's calculations [11] are presented in Figures 1 and 2. Note, that at present no other theoretical or experimental results are available for comparison of the proton rate coefficients. It is possible to compare the proton collision excitation with electron one. In Figures 1 and 2 the electron excitation rate coefficients calculated by extrapolation of data of Aggarwal & Keenan [13] in the low energy region are presented. It should be noted that designations of energy levels used in paper [13] (namely,  $^3P_2$ ,  $^1P_1$ ,  $^3P_0$ ,  $^3P_1$ , ordered by increasing level energy) differ from the designations used in paper [11] (namely,  $^3P_2$ ,  $^3P_1$ ,  $^3P_0$ ,  $^1P_1$ , ordered by increasing level energy). Landman used intermediate-coupling terms converted from LS-coupling terms by using the adopted transformation coefficient which was given in his table 2. Our presentation of proton rate coefficients in Figs. 1, 2 and in Table 1 corresponds to the designations of Aggarwal & Keenan. One can see from Figs. 1 and 2 that in the region  $T \geq 10^7$  K proton collisions are important for all levels considered (where it is assumed that proton temperature is equal to electron temperature).

We fitted data of Ref. [11] by formula (3), and obtained values of fitting parameters  $\rho_i$  are presented in Table 1.

It should be noted that proton collisions can not effectively excite  $2s^22p^53s$  levels from the ground level  $2s^22p^6$   $^1S_0$ . However, the  $2s^22p^53s$   $^3P_2$  and  $^3P_0$  levels are metastable and can have substantial population densities at relatively low density plasma. Therefore, proton collisions can play a significant role at densities where collision depopulation of these levels competes with their radiative decay. Under such conditions, for example, the relative intensities of the  $2s^22p^53s$   $^3P_0 - 2s^22p^53s$   $^3P_1$  M1 (115.32nm) and  $2s^22p^53s$   $^3P_2 - 2p^6$   $^1S_0$  M2 (1.7097nm) lines relative to the  $2s^22p^53s$   $^3P_1 - 2s^22p^6$   $^1S_0$  line (1.6777nm) may provide useful density diagnostics [11]. Because radiative probabilities  $A(2s^22p^53s$   $^3P_0 - 2s^22p^53s$   $^3P_1) = 1.6 \times 10^4$  s<sup>-1</sup>,  $A(2s^22p^53s$   $^3P_0 - 2s^22p^53s$   $^3P_2) \sim 2$  s<sup>-1</sup>,

$A(2s^22p^53s\ ^3P_2 - 2s^22p^6\ ^1S_0) = 2.0 \times 10^5\ \text{s}^{-1}$  (see, for example, [11] and NIST database<sup>1</sup>), data presented in Figures 1 and 2 and condition (2) follows that proton collision decay will be important for  $2s^22p^53s\ ^3P_0$  level at  $N_p \geq 10^{12}\ \text{cm}^{-3}$  and for  $2s^22p^53s\ ^3P_1$  level at  $N_p \geq 10^{15}\ \text{cm}^{-3}$ . Note that CHIANTI [6], an atomic database for spectroscopic diagnostics of astrophysical plasmas, does not use proton impact excitation data.

### F-like Fe XVIII ion ( $2s^22p^5\ ^2P_{3/2} - ^2P_{1/2}$ )

Several semiclassical calculations, with both first-order and close-coupling approximation, have been performed for Fe XVIII ion. The first-order semiclassical calculations were done by Kastner & Bhatia [14] and some later by Feldman *et al.* [15].

The close-coupling semiclassical method of Reid and Schwarz [16] has been used by several authors to calculate both proton collision excitation cross sections and rate coefficients for the  $2s^22p^5\ ^2P_{3/2} - ^2P_{1/2}$  transition in Fe XVIII [17 - 19]. In earlier paper [17] such aspects as polarization effects, symmetrization of coupled equations, or departures from LS-coupling were not considered. Later Keenan and Reid [18] developed this method to incorporate symmetrization with respect to channel velocities, and in a further development, Foster *et al.* [19] improved the accuracy of the calculations by considering both symmetrization and polarization effects, whereby they have included the  $2s2p^6\ ^2S_{1/2}$  level by means of a polarization potential. The inclusion of such factors has resulted in a difference of 60% comparing to the cross sections by [18] (see Fig.3).

The importance of including polarization effects in intramultiplet excitation collisions was noted in papers [8, 9] where quantum molecular approach was used to describe the proton-ion interaction. In calculations [19], the polarization was taken into account by the inclusion of the  $2s2p^6\ ^2S_{1/2}$  state alone. For Fe XVIII ion the major component of the polarization can be really incorporated by a single state, because the next states that contribute to the polarization (i.e., states with configuration  $2s^22p^43s$ ) have about 6 times larger excitation energies than  $2s2p^6$ . This is a feature of highly charged F-like systems and, generally speaking, one would not expect that a single state could give a good representation of the polarization in general case.

Excitation rate coefficients obtained in papers [14, 15, 18, 19] are presented in Fig. 4. Note that results from [19] are smaller than the semiempirical results of [14, 15] by more than a factor of 2, over the small temperature range for which they presented results, and are 30-36% lower than the results by [18], where the effects of the  $^2S$  state were not included. We recommend to use data of [19], and show corresponding values

<sup>1</sup> NIST Atomic Spectra Database <http://physics.nist.gov/PhysRefData/ASD/index.html>

of fitting parameters in Table 1.

Extrapolated excitation rate coefficient by electron impact obtained in [20] for the transition  $2s^22p^5 \ ^2P_{3/2} - ^2P_{1/2}$  is about  $(1-2) \times 10^{-9} \text{ cm}^3\text{s}^{-1}$  in the temperature region  $T \sim (2-6) \times 10^7 \text{ K}$ . It means that in plasma with  $T_e = T_p$  excitation by proton impact can increase the population of  $2s^22p^5 \ ^2P_{1/2}$  level only by 10%. Of course, at  $T_e \neq T_p$  the influence of proton excitation may be more important.

Note also that the critical density (1) for transition considered is about  $10^{14} \text{ cm}^{-3}$  (see, for example, [19]). It indicates that proton excitation process may be important for Fe XVIII ion only in the low density plasma with  $N_e \leq 10^{14} \text{ cm}^{-3}$ .

Foster *et al.* [19] used their proton excitation rates to calculate intensity ratio R for spectral lines  $2s^22p^5 \ ^2P_{3/2} - 2s^22p^5 \ ^2P_{1/2}$  and  $2s^22p^5 \ ^2P_{3/2} - 2s2p^6 \ ^2S_{1/2}$  at plasma parameters determined independently in the experiment on the JIPP T-II-U tokamak (Nagoya, Japan), and compared these calculations with results observed by Sato *et al.* [21]. One can see from Fig. 5 that modeling results agreed very well with experimental ones.

CHIANTI database uses data of Ref. [19].

### O-like Fe XIX ion ( $2s^22p^4 \ ^3P_J - ^3P_J$ )

There is only one paper by Feldman *et al.* [15] where data on proton excitation of  $^3P_2 - ^3P_0$  and  $^3P_2 - ^3P_1$  transitions in O-like Fe XIX ion were calculated by first-order semiclassical method and data are presented for one temperature value.

There are unpublished data calculated by Ryans *et al.* [22] by using of semiclassical close-coupling approach of Reid & Schwarz [16]. These data now are used in CHIANTI database [6] and just these data have been fitted to formula (3) in the present work.

In Figures 6, 7 and 8 we present results of our fitting together with proton excitation rates calculated in [15, 22] and results of calculation of the electron excitation rate coefficients obtained by Butler & Zeippen [23]. It can be seen from Figs. 6, 7 that proton-ion collisions will influence strongly on population of  $^3P_0$  and  $^3P_1$  levels at practically all reasonable values of temperature. It is interesting, that electron rate coefficient for  $^3P_0 - ^3P_1$  transition (not presented in Fig.8) is higher than proton one on about 2 orders. The electron collision excitation rate coefficient for  $^3P_0 - ^3P_1$  transition is about  $2 \times 10^{-10} \text{ cm}^3\text{s}^{-1}$  at temperature about  $3 \times 10^6 \text{ K}$  and  $8 \times 10^{-11} \text{ cm}^3\text{s}^{-1}$  at  $T_e \sim 10^7 \text{ K}$  [23]. It means that collision mixing of  $^3P_0$  and  $^3P_1$  levels will be occurred by only electron-ion collisions. The probabilities of radiative decay for levels  $^3P_0$  and  $^3P_1$  are [24]:  $A(^3P_0 - ^3P_2) =$



$0.53 \text{ s}^{-1}$ ,  $A(^3P_1-^3P_2) = 1.43 \times 10^4 \text{ s}^{-1}$ , and  $A(^3P_1-^3P_0) = 30.5 \text{ s}^{-1}$ . In plasma with  $N_e \gg 3 \times 10^{14} \text{ cm}^{-3}$  electrons will cause Boltzmann equilibrium among fine-structure levels and proton collision will not be important for the ion kinetics.

### **N-like Fe XX ion ( $2s^2 2p^3 \ ^4S_{3/2}, \ ^2D_{3/2,5/2}, \ ^2P_{1/2,3/2}$ )**

At present time there is only one paper where Bhatia & Mason [25] have used the semiclassical first-order method of Bely and Faucher [26] to calculate proton impact excitation of fine-structure transitions in Fe XX ion. We fitted these data to formula (3) and obtained results are presented in Table 1. In Figures 9-11 the temperature dependencies of proton excitation rates are shown together with electron excitation rates calculated by Butler & Zeppen [27]. It can be seen that for practically all transitions (except  $^4S_{3/2} - ^2P_{1/2,3/2}$ ) proton rate coefficients are comparable or larger than electron ones at all reasonable temperatures. The density region where proton collisions are important for population kinetics of fine-structure levels can be estimated from equation (2) by using radiative probabilities calculated in paper [25]. Because total radiative decay probabilities are  $A(^2D_{3/2}) = 1.56 \times 10^4 \text{ s}^{-1}$ ,  $A(^2D_{5/2}) = 1.68 \times 10^3 \text{ s}^{-1}$ ,  $A(^2P_{1/2}) = 3.53 \times 10^4 \text{ s}^{-1}$ , and  $A(^2P_{3/2}) = 8.05 \times 10^4 \text{ s}^{-1}$ , we obtain that it is necessary to take into account proton collisions in kinetic calculations for plasma with electron density  $N_e \leq 10^{16} \text{ cm}^{-3}$ .

CHIANTI database uses data of Ref. [25].

### **C-like Fe XXI ion ( $2s^2 2p^2 \ ^3P_J - ^3P_J$ )**

Several calculations by both semiclassical and quantum methods have been performed for ground configuration of Fe XXI ion.

The close-coupling semiclassical calculations were done by Ryans et al. [28, 29]. They considered  $^3P_0-^3P_1$ ,  $^3P_0-^3P_2$  and  $^3P_1-^3P_2$  transitions among the fine-structure levels  $2s^2 2p^2 \ ^3P_J$  of carbon-like Fe (Fe XXI) ion and calculated the proton rates using the symmetrized close-coupling semi-classical approach in which the interaction matrix elements were modified to give them the correct short-range forms, and the effects of dipole coupling to nearby terms were included by means of a polarization potential. It was selected a set of excited terms which are coupled to the ground state by the E1 interaction. In the present case of  $^3P$  ground state, the terms that can contribute to the polarization have symmetry  $^3S$ ,  $^3P$ , or  $^3D$ . Therefore calculations in paper [28] were made in two approximations: 1) when only the three excited terms  $2s2p^3 \ ^3D$ ,  $^3P$ , and  $^3S$  were included in the calculation via the polarization potential and 2) when the terms  $2s^2 2p3s \ ^3P$  and  $2s^2 2p3d \ ^3D$ ,  $^3P$  were also included to test the convergence of the results. It was shown

that, for Fe XXI ion, and for protons as perturbers, the inclusion of the further excited terms had a small effect on the cross sections. For the Fe XXI ion, as well as for other heavy ions, the polarization affects the cross sections significantly at all impact energies. However, for the heavy ions the polarization potential is dominated by the  $2s2p^3$  terms, because the excitation energies of the  $2s^22p3l$ ,  $2s2p^23l$ , and higher configurations are much larger than the excitation energies of  $2s2p^3$ . It means that the representation of polarization by the  $2s2p^3$  terms is adequate to calculate  $2s^22p^2\ ^3P_J\text{-}^3P_{J'}$  transitions in Fe XXI ion. Note that additional including of  $2p3l$  terms do not allow to increase calculation accuracy, because in this case including some others configurations (for example,  $2s2p^23p$ ) are also needed. The results of calculations [29] where only  $2s2p^3$  configuration were taken into account for polarization potential are shown in Figures 12-14. Note also, that in the low energy tail of the cross sections, where close-coupling calculations are difficult, first-order cross sections, modified to allow for polarization were used in calculations of proton rates coefficients by Ryans et al. [29]. These rate coefficients were fitted to formula (3) and results obtained are presented in Table 1. Note that CHIANTI database uses data of Ref. [29].

Earlier Faucher [30] considered proton-impact excitation of C-like Fe XXI using a quantum formulation. For Fe XXI the differences between results of [30] and [29] are essential, especially for the  $^3P_0\text{-}^3P_1$  transition (see Figs. 12-14). In Faucher's calculations electrostatic interaction potential was approximated by its long range quadrupole part and no polarization effects were taken into account. Ryans et al. [28] made special calculation with the polarization omitted using the same atomic data as Faucher [30]. This calculation differs from [30] only in two respects: 1) in the collision treatment – semiclassical versus quantum, 2) in the interaction between matrix elements – short-range modified forms versus purely asymptotic forms. For  $^3P_0\text{-}^3P_2$  and  $^3P_1\text{-}^3P_2$  transitions these results are close to [30] in the energy region  $E_p < 3$  KeV, and for higher energies the progressive divergence in the two calculations is due to difference in the short-range part of interaction potential. For the  $^3P_0\text{-}^3P_1$  transition the discrepancy is larger because the strictly second-order process is more sensitive to the short-range forms of the matrix elements [28]. Thus, in calculations [30] two important effects (modification of interaction potential at short distances and polarization) were not taken into account, and we recommend to use data of [29].

Comparisons of proton and electron excitation rates are also shown in Figs. 12-14. It is clearly seen that only for transition  $^3P_0\text{-}^3P_1$  proton collisions are not important, while for other transitions  $^3P_0\text{-}^3P_2$  and  $^3P_1\text{-}^3P_2$  proton rates dominate. According to the paper

[24] total probabilities of radiative decay of  ${}^3P_1$  and  ${}^3P_2$  levels are:  $A({}^3P_1) = 6.52 \times 10^3 \text{ s}^{-1}$ ,  $A({}^3P_2) = 1.04 \text{ s}^{-1}$ . It means (see equation (2)), that in plasma with  $N_e \gg 10^{15} \text{ cm}^{-3}$  electrons will cause Boltzmann equilibrium among fine-structure levels and proton collision will not be important for ion kinetics.

### **B-like Fe XXII ion ( $2s^2 2p^2 {}^2P_J - {}^2P_{J'}$ , $2s 2p^2 {}^4P_J - {}^4P_{J'}$ )**

At present time for B-like Fe XXII there are only calculations made by Foster et al. [32-34]. In these papers cross sections and excitation rate coefficients for fine-structure transitions within both the ground  $2s^2 2p^2 {}^2P$  and the metastable  $2s 2p^2 {}^4P$  terms have been obtained. All calculations used the semiclassical symmetrized, close-coupling method of Reid and Schwarz [16], modified to include higher lying levels by means of a polarization potential. In the former case [32], the  $2s 2p^2 {}^2S$ ,  ${}^2P$ ,  ${}^2D$  terms were included, while in the latter [33, 34], the  $2p^3 {}^4S^\circ$  term was also included. Additionally, in these calculations the interaction matrix elements were modified to give them the correct short-range forms. The values of the magnitudes of the required matrix elements were derived from the best available oscillator strengths, while the signs of matrix elements were taken to be those that would arise from LS-coupled hydrogenic orbitals. It means that errors might arise if the ion departs too far from LS-coupling. Therefore Foster et al. [34] estimates accuracy of their data for Fe XXII to be 30% in the high temperature region. We have fitted data [34] to formula (3) and the values of fitting parameters are presented in Table 1. CHIANTI database uses data of Ref. [34].

In Figures 15 and 16 the temperature dependence of the proton excitation rates are shown together with data of [35] for the electron excitation rates. It is seen that for the transitions  $2s^2 2p^2 {}^2P_{1/2} - {}^2P_{3/2}$ ,  $2s 2p^2 {}^4P_{1/2} - {}^4P_{5/2}$  and  $2s 2p^2 {}^4P_{3/2} - {}^4P_{5/2}$  proton collisions dominate at practically all reasonable temperatures, and for the  $2s 2p^2 {}^4P_{1/2} - {}^4P_{3/2}$  transition the proton collisions are important at  $T > 10^7 \text{ K}$ .

According to the paper [24] total probabilities of radiative decay of levels considered are:  $A(2s^2 2p^2 {}^2P_{3/2}) = 1.48 \times 10^4 \text{ s}^{-1}$ ,  $A(2s 2p^2 {}^4P_{1/2}) = 0.97 \times 10^8 \text{ s}^{-1}$ ,  $A(2s 2p^2 {}^4P_{3/2}) = 1.02 \times 10^7 \text{ s}^{-1}$ ,  $A(2s 2p^2 {}^4P_{5/2}) = 0.67 \times 10^8 \text{ s}^{-1}$ . It means that proton collisions will be effectively populate  $2s^2 2p^2 {}^2P_{3/2}$  level at plasma densities  $N_e < 10^{16} \text{ cm}^{-3}$  (see (1)), and effectively influence on populations of  $2s 2p^2 {}^4P_{1/2,3/2,5/2}$  levels at  $N_p > 10^{16} \text{ cm}^{-3}$  (see (2)). So, in this case it is necessary to take proton excitation processes into account in both low and high dense plasma.

### **Be-like Fe XXIII ion ( $2s 2p^3 {}^3P_J - {}^3P_{J'}$ )**

Excitation of FeXXIII levels from the ground state by proton impact is not important because the energy difference between the first excited configuration  $2s2p$  and the ground configuration  $2s^2$  is large. However the first excited configuration contain a closely spaced metastable levels  $2s2p\ ^3P_J$  for which proton-induced transitions can be important. There are several papers concerning with calculation of proton rates for these transitions.

Feldman et al. [15] used first-order semiclassical approach (see above) and present proton rate only at one temperature value.

More sophisticated calculations based on semiclassical close-coupling method were carried out by Doyle [36]. The calculations were split into two energy ranges: a low-energy and intermediate-energy ranges. For both energy ranges, the perturbing proton follows a classical Coulomb trajectory, but for the first range first-order theory was used and close-coupling equations were solved only for the second region. Calculations were carried out with different short-range forms of interaction matrix elements but no polarization effects have been taken into account.

The importance of including the effects of higher-lying states in the calculation of proton rates via a polarization potential technique was demonstrated by Foster et al. [19] and Ryans et al. [28, 29] for the ground term fine-structure transitions in F-like and B-like ions. In paper [37] Ryans et al. extended this approach to Be-like ions and calculated proton excitation cross sections and rate coefficients for transitions among the  $1s^22s2p\ ^3P$  fine-structure levels of Fe XXIII. The cross sections for transitions  $2s2p\ ^3P_J - ^3P_{J'}$ , were calculated by the same symmetrized close-coupled semiclassical treatment that we have described above (F-like and B-like Fe ions): the interaction matrix elements are modified to have the correct short-range forms and the effects of dipole coupling to nearby terms are included by means of a polarization potential. In the case of Fe XIII ion dipole coupling to the  $2p^2\ ^3P$ ,  $2s3s\ ^3S$ , and  $2s3d\ ^3D$  terms were included in the polarization potential. Ryans et al. [37] estimates accuracy of their data for Fe XXII to be 20%. We have fitted data [37] to formula (3) and the values of fitting parameters are presented in Table 1. CHIANTI database uses data of Ref. [37].

In Figure 17 temperature dependence of proton excitation rates calculated in papers [15, 36, 37] are shown together with data of [38] for electron excitation rates. It is seen that proton collision are very important for transitions  $2s2p\ ^3P_0 - ^3P_2$ ,  $2s2p\ ^3P_1 - ^3P_2$  at  $T > 10^7$  K and are not important for transition  $2s2p\ ^3P_0 - ^3P_1$  at practically all reasonable temperatures.

Among the components of  $2s2p\ ^3P$  term, level  $^3P_1$  has the largest probability of radiative decay:  $A(2s2p\ ^3P_1 - 2s^2\ ^1S_0) = 4.91 \times 10^7\ s^{-1}$  [24]. It means that in plasma with  $N_e >$

$10^{18} \text{ cm}^{-3}$  electron collisions can cause Boltzmann population distribution among  $2s2p^3P$  term. In lower density plasma it is necessary to take the proton excitation processes into account in radiative-collision kinetic calculations.

### 3. Summary

In the present work we evaluated the data for proton-induced transitions in Fe XVII – Fe XXIII ions which were obtained with different theoretical methods. It is used a simple analytical formula with 7 parameters allowing to describe dependence of proton rate coefficient on proton temperature in a wide temperature range. The values of free parameters have been determined by fitting numerical data to an analytical formula and are presented as recommended data together with fitting accuracies. The results obtained can be used for plasma kinetic calculations and for development of spectroscopy methods of plasma diagnostics.

### Acknowledgement

This work was performed when I. Skobelev was a visiting professor of National Institute for Fusion Science from Sep. 2005 to Jan. 2006.

### References

1. M. J. Seaton, *Mon. Not. R. Astron. Soc.*, **127**, 191 (1964)
2. I. Skobelev, I. Murakami, T Kato, (to be published)
3. A. Dalgarno, in *Atoms in Astrophysics*, edited by P. G. Burke, W. B. Eissner, D. G. Hummer, and I. C. Percival (Plenum Press, New York, 1983), p. 103
4. R. H. G. Reid, *Adv. At. Mol. Phys.*, **25**, 251 (1988)
5. F. Copeland, R. H. G. Reid, F. P. Keenan, *ADNDT*, **67**, 179 (1997)
6. P. R. Young, G. Del Zanna, E. Landi, K. P. Dere, H. E. Mason, M. Landini, *Astrophys. J. Suppl.*, **144**, 135 (2003)
7. K. Alder, A. Bohr, T. Huus, B. Mottleson, and A. Winther, *Rev. Mod. Phys.*, **28**, 432 (1956)
8. T. G. Heil, S. Green, and A. Dalgarno, *Phys. Rev. A*, **26**, 3293 (1982)
9. T. G. Heil, K. Kirby, and A. Dalgarno, *Phys. Rev. A*, **27**, 2826 (1983)
10. P. Faucher, D. A. Landman, *Astron. Astrophys.*, **54**, 159 (1977)
11. D. A. Landman, *JQSRT*, **34**, 365 (1985)

12. C Froese Fischer, *Comp. Phys. Comm.*, **14**, 145 (1978).
13. K. M. Aggarwal, F. P. Keenan, A. Z. Msezane, *Ap.J. Suppl.*, **144**, 169 (2003)
14. S. O. Kastner and A. K. Bhatia, *Astron. Astrophys.*, **71**, 211(1979).
- 15 U. Feldman, G. A. Doschek, Chung-Chieh Cheng, A. K. Bhatia, *J. Appl. Phys.*, **51**, 190 (1980)
16. R. H. G. Reid and J. H. Schwarz, in *Proceedings of the Sixth International Conference on Physics of Electronic and Atomic Collisions*, Cambridge, MA, edited by I. Amdur (MIT, Cambridge, MA, 1969), p. 236.
17. F. P. Keenan and R. H. G. Reid, *J. Phys. B* **20**, L753 (1987).
18. F. P. Keenan and R. H. G. Reid, *J. Phys. B* **22**, L295 (1989).
19. V. J. Foster, F. P. Keenan, R. H. G. Reid, *Phys. Rev. A.*, **49**, 3092 (1994).
20. D. G. Hummer, K. A. Berrington; W. Eissner, A. K. Pradhan, H. E. Saraph, J. A. Tully, *A&A*, **279**, 298 (1993)
21. K. Sato, M. Mimura, M. Ostuka, T. Watari, M. Ono, K. Toi, Y. Kawasumi, K. Kawahata, and T. Oda, *Phys. Rev. Lett.*, **56**, 151 (1986).
22. R. S. I. Ryans, F. P. Keenan, R. H. G. Reid, unpublished
23. K. Butler and C. J. Zeippen, *A&A*, **372**, 1083 (2001).
24. T. Cheng, Y.-K. Kim, J.P. Desclaux, *ADNDT*, **24**, 111 (1979)
- 25 A. K. Bhatia, H. E. Mason, *A&A*, **83**, 380 (1980)
26. O. Bely, P. Faucher, *A&A*, **6**, 88 (1970)
27. K. Butler and C. J. Zeippen, *A&A*, **372**, 1078 (2001).
28. R. C. I. Ryans, V. J. Foster-Woods, R. H. G. Reid, F. P. Keenan, *A&A*, **345**, 663 (1999)
29. R. C. I. Ryans, V. J. Foster-Woods, F. P. Keenan, R. H. G. Reid, *ADNDT*, **73**, 1 (1999)
30. P. Faucher, *A&A*, **54**, 589 (1977)
31. K. Butler and C. J. Zeippen, *A&AS*, **143**, 483 (2000)
32. V. J. Foster, F. P. Keenan, R. H. G. Reid, *A&A*, **308**, 1009 (1996)
33. V. J. Foster, R. H. G. Reid, F. P. Keenan, *MNRAS*, **288**, 973 (1997)
34. V. J. Foster, F. P. Keenan, R. H. G. Reid, *ADNDT*, **67**, 99 (1997)
35. H. L. Zhang, A. K. Pradhan, *A&AS* **123**, 575 (1997)
36. J.G. Doyle, *ADNDT*, **37**, 441 (1987)
37. R.S.I. Ryans, V. J. Foster-Woods, F. Copeland, F. P. Keenan, A. Matthews, R. H. G. Reid, *ADNDT*, **70**, 179 (1998)
38. M. C. Chidichimo, G. Del Zanna, H. E. Mason, N. R. Badnell, J. A. Tully, K. A. Berrington, *A&A*, **430**, 331 (2005)

Table 1. The values of approximation parameters for proton excitation rate coefficients for transitions in ions Fe XVII – Fe XXIII.

Ref.	Ion	Transition	Approximation parameters							Accuracy of approximation, %
			$\rho_1$	$\rho_2$	$\rho_3$	$\rho_4$	$\rho_5$	$\rho_6$	$\rho_7$	
[11]	Fe XVII	$2s^2 2p^5 3s^3 P_2 - 2s^2 2p^5 3s^1 P_1$	0.0252	1	1	290	2.2	100	2.5	3 (for $T_p$ 170-1100 eV)
[11]	Fe XVII	$2s^2 2p^5 3s^3 P_2 - 2s^2 2p^5 3s^3 P_1$	0.069	214	2	567	1.94	200	2.1	1.8 (for $T_p$ 200-1100 eV)
[11]	Fe XVII	$2s^2 2p^5 3s^3 P_2 - 2s^2 2p^5 3s^3 P_0$	0.0638	220	2	490	1.87	200	2.1	3 (for $T_p$ 200-1100 eV)
[11]	Fe XVII	$2s^2 2p^5 3s^1 P_1 - 2s^2 2p^5 3s^3 P_1$	0.197	219	2	439	1.77	200	2.1	2.6 (for $T_p$ 200-1100 eV)
[11]	Fe XVII	$2s^2 2p^5 3s^1 P_1 - 2s^2 2p^5 3s^3 P_0$	0.003	247	2	790	2.35	200	2.1	2.3 (for $T_p$ 200-1100 eV)
[11]	Fe XVII	$2s^2 2p^5 3s^3 P_0 - 2s^2 2p^5 3s^3 P_1$	0.0205	249	2.1	870	2.6	250	2.1	2.7 (for $T_p$ 200-1100 eV)
[19]	Fe XVIII	$2s^2 2p^5^2 P_{3/2} - 2s^2 2p^5^2 P_{1/2}$	0.00109	189	2	743	2.33	38	2.29	2.9 (for $T_p$ 170-3500 eV)
[22]	Fe XIX	$2s^2 2p^4^3 P_2 - 2s^2 2p^4^3 P_0$	0.00945	150	2.5	630	2.66	150	2.8	4 (for $T_p = 150-3100$ eV)
[22]	Fe XIX	$2s^2 2p^4^3 P_2 - 2s^2 2p^4^3 P_1$	0.005	165	2	649	2.62	150	2.8	3.7 (for $T_p = 150-3100$ eV)
[22]	Fe XIX	$2s^2 2p^4^3 P_0 - 2s^2 2p^4^3 P_1$	0.000785	70	1.4	175	2.33	25	2.0	1.4 (for $T_p = 150-3100$ eV)
[25]	Fe XX	$2s^2 2p^3^4 S_{1/2} - 2s^2 2p^3^2 D_{3/2}$	0.35	720	1.3	1287	15	670	0.9	1.2 (for $T_p = 500-1300$ eV)
[25]	Fe XX	$2s^2 2p^3^4 S_{1/2} - 2s^2 2p^3^2 D_{5/2}$	0.5	689	1.3	3250	3	670	1.05	1.6 (for $T_p = 500-1300$ eV)
[25]	Fe XX	$2s^2 2p^3^4 S_{1/2} - 2s^2 2p^3^2 P_{1/2}$	0.0675	1000	0.05	1160	4.8	800	4	4.8 (for $T_p = 700-1300$ eV)
[25]	Fe XX	$2s^2 2p^3^4 S_{1/2} - 2s^2 2p^3^2 P_{3/2}$	0.00488	1000	0.05	1200	4	800	4	2.5 (for $T_p = 500-1300$ eV)
[25]	Fe XX	$2s^2 2p^3^2 D_{3/2} - 2s^2 2p^3^2 D_{5/2}$	2.16	500	1.3	1500	0.7	670	0.8	2.8 (for $T_p = 500-1300$ eV)
[25]	Fe XX	$2s^2 2p^3^2 D_{3/2} - 2s^2 2p^3^2 P_{1/2}$	2.2	500	1.33	1020	1.1	670	1.3	2.8 (for $T_p = 500-1300$ eV)

[25]	Fe XX	$2s^2 2p^3 \ ^2D_{3/2} - 2s^2 2p^3 \ ^2P_{3/2}$	0.48	550	1.7	4000	1.0	670	1.3	1.3 (for $T_p = 500-1300$ eV)
[25]	Fe XX	$2s^2 2p^3 \ ^2D_{5/2} - 2s^2 2p^3 \ ^2P_{1/2}$	1.64	550	1.0	1100	0.4	500	1.0	1.9 (for $T_p = 500-1300$ eV)
[25]	Fe XX	$2s^2 2p^3 \ ^2D_{5/2} - 2s^2 2p^3 \ ^2P_{3/2}$	1.52	555	1.25	13000	0.5	500	1.0	2.1 (for $T_p = 500-1300$ eV)
[25]	Fe XX	$2s^2 2p^3 \ ^2P_{1/2} - 2s^2 2p^3 \ ^2P_{3/2}$	2.82	700	1.0	670	0.45	500	0.75	1.3 (for $T_p = 500-1300$ eV)
[29]	Fe XXI	$2s^2 2p^3 \ ^3P_0 - 2s^2 2p^3 \ ^3P_1$	$6.7 \times 10^{-6}$	500	1.52	1875	2.05	0.5	1.2	5 (for $T_p = 250-8500$ eV)
[29]	Fe XXI	$2s^2 2p^3 \ ^3P_0 - 2s^2 2p^3 \ ^3P_2$	0.585	530	1.35	2400	1.37	260	0.85	5 (for $T_p = 250-8500$ eV)
[29]	Fe XXI	$2s^2 2p^3 \ ^3P_1 - 2s^2 2p^3 \ ^3P_2$	0.75	510	1.0	1400	1.3	260	0.75	3.5 (for $T_p = 170-13000$ eV)
[34]	Fe XXII	$2s^2 2p^2 \ ^2P_{1/2} - 2s^2 2p^2 \ ^2P_{3/2}$	0.815	720	1.01	1100	1.66	330	1.24	4.4 (for $T_p = 130-8600$ eV)
[34]	Fe XXII	$2s^2 2p^2 \ ^4P_{1/2} - 2s^2 2p^2 \ ^4P_{3/2}$	0.03	340	1.11	1070	1.79	260	1.47	4.8 (for $T_p = 77-5200$ eV)
[34]	Fe XXII	$2s^2 2p^2 \ ^4P_{1/2} - 2s^2 2p^2 \ ^4P_{5/2}$	0.475	478	1.125	960	1.92	500	1.7	4.4 (for $T_p = 100-5200$ eV)
[34]	Fe XXII	$2s^2 2p^2 \ ^4P_{3/2} - 2s^2 2p^2 \ ^4P_{5/2}$	0.21	326	1.15	910	1.47	260	1.47	4.5 (for $T_p = 86-5200$ eV)
[37]	Fe XXIII	$2s^2 2p^3 \ ^3P_0 - 2s^2 2p^3 \ ^3P_1$	0.007	945	1.01	1345	1.99	330	1.24	4 (for $T_p = 170-9000$ eV)
[37]	Fe XXIII	$2s^2 2p^3 \ ^3P_0 - 2s^2 2p^3 \ ^3P_2$	0.69	922	0.97	858	1.5	330	1.1	3.3 (for $T_p = 170-17000$ eV)
[37]	Fe XXIII	$2s^2 2p^3 \ ^3P_1 - 2s^2 2p^3 \ ^3P_2$	0.62	860	0.92	770	1.55	330	1.15	2.1 (for $T_p = 170-13000$ eV)



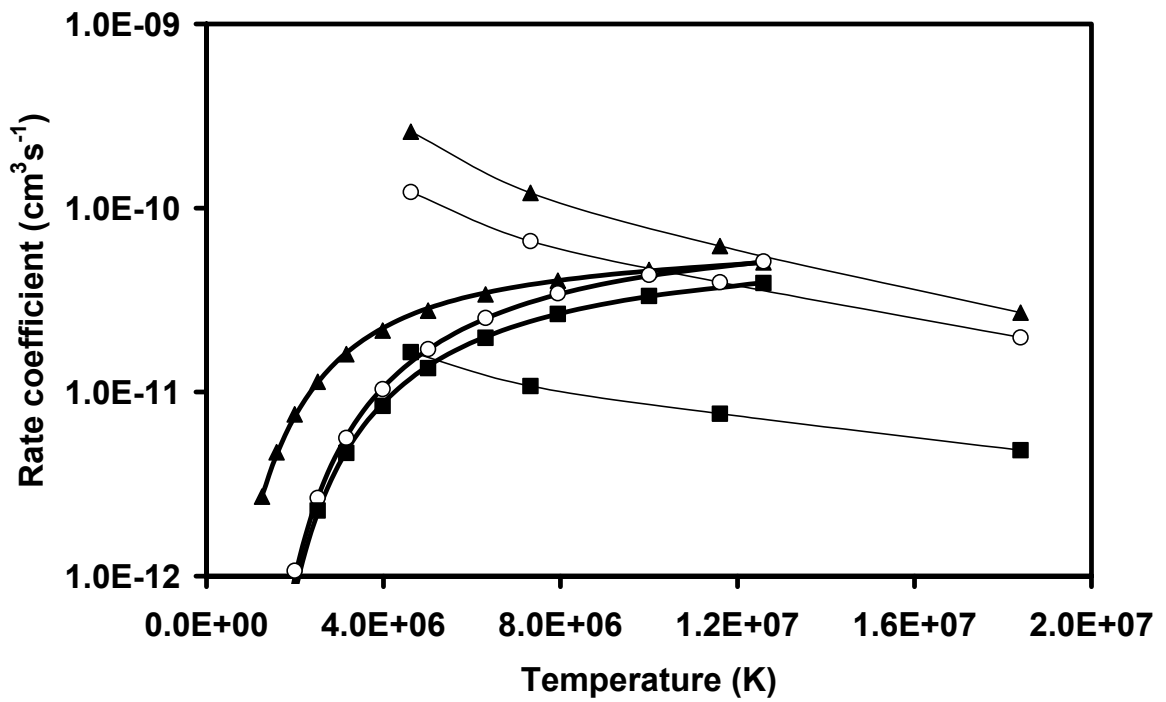


Figure 1. Collision rate coefficient for transition  $2s^22p^53s \ ^3P_2 - \ ^3P_J$  in Ne-like Fe XVII: solid thick lines – formula (3) for proton impact, solid thin lines – electron impact [13],  $\blacktriangle$  – data [11,13] for level  $^1P_1$ ,  $\blacksquare$  – data [11,13] for level  $^3P_0$ ,  $\circ$  – data [11,13] for level  $^3P_1$ .

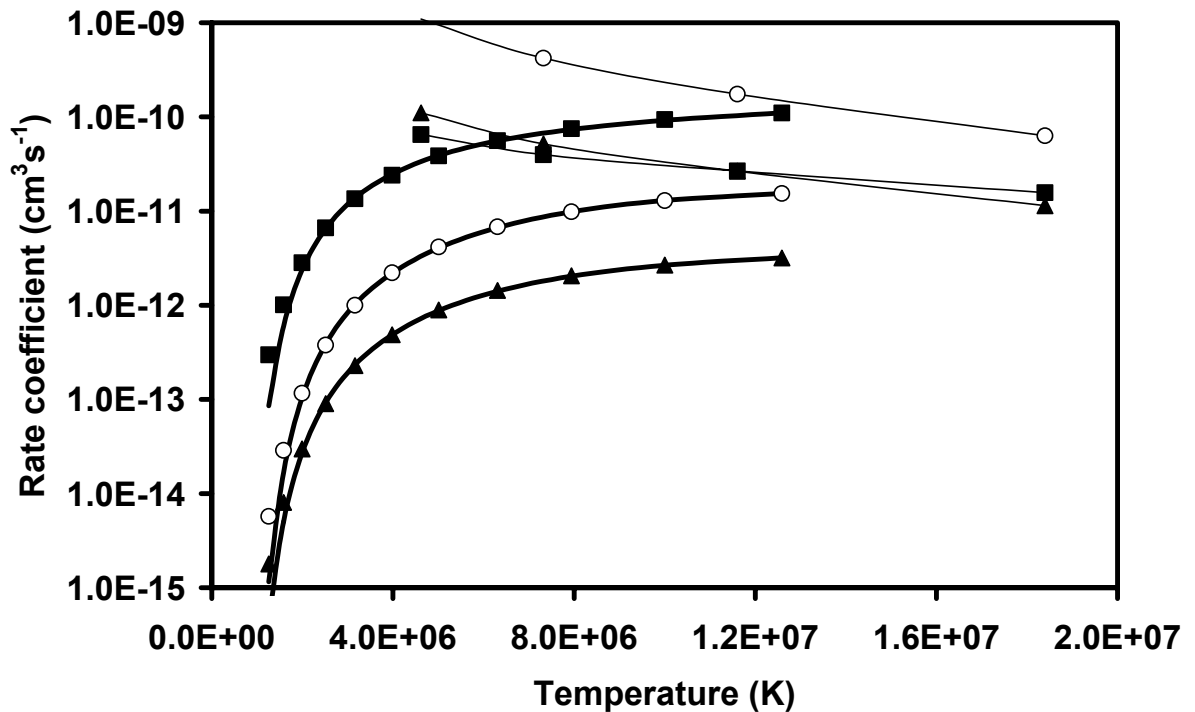


Figure 2. Collision rate coefficient for transition  $2s^22p^53s \ ^3P_J - \ ^3P_J$  in Ne-like Fe XVII: solid thick lines – formula (3) for proton impact, solid thin lines – electron impact [13],  $\blacktriangle$  – data [11,13] for transition  $^1P_1-^3P_0$ ,  $\blacksquare$  – data [11,13] for transition  $^1P_1-^3P_1$ ,  $\circ$  – data [11,13] for transition  $^3P_0-^3P_1$ .

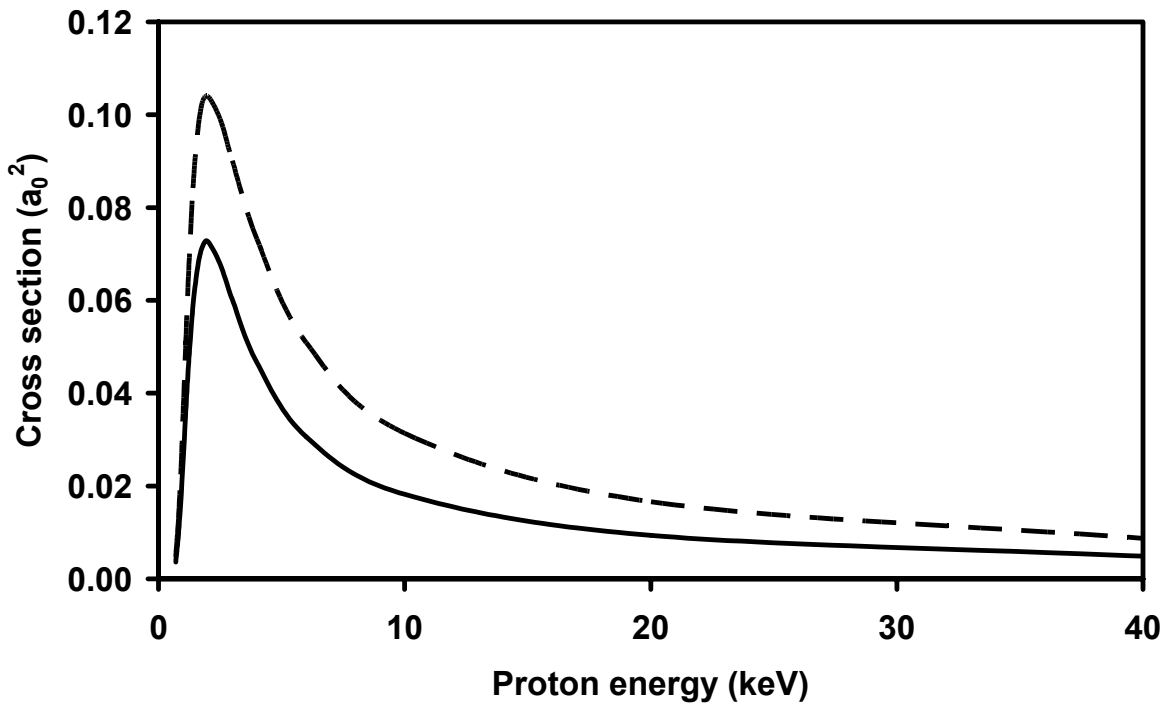


Figure 3. Proton collision cross section for transition  $2s^2 2p^5 \ ^2P_{3/2} - \ ^2P_{1/2}$  in F-like Fe XVIII: solid line – data [19], dashed line – data [18].

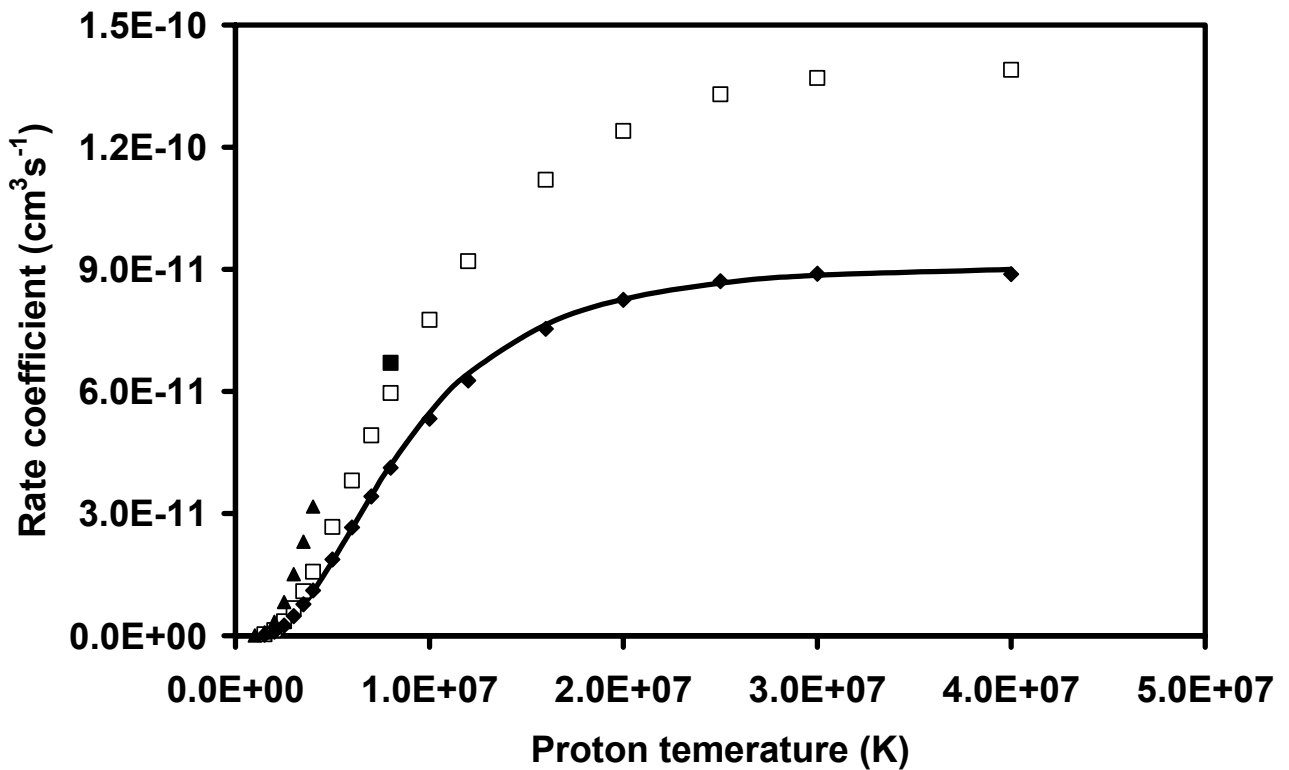


Figure 4. Proton collision rate coefficient for transition  $2s^2 2p^5 \ ^2P_{3/2} - \ ^2P_{1/2}$  in F-like Fe XVIII: solid line – formula (3),  $\blacklozenge$  - data [19],  $\square$  – data [18],  $\blacktriangle$  - data [14],  $\blacksquare$  - data [15].

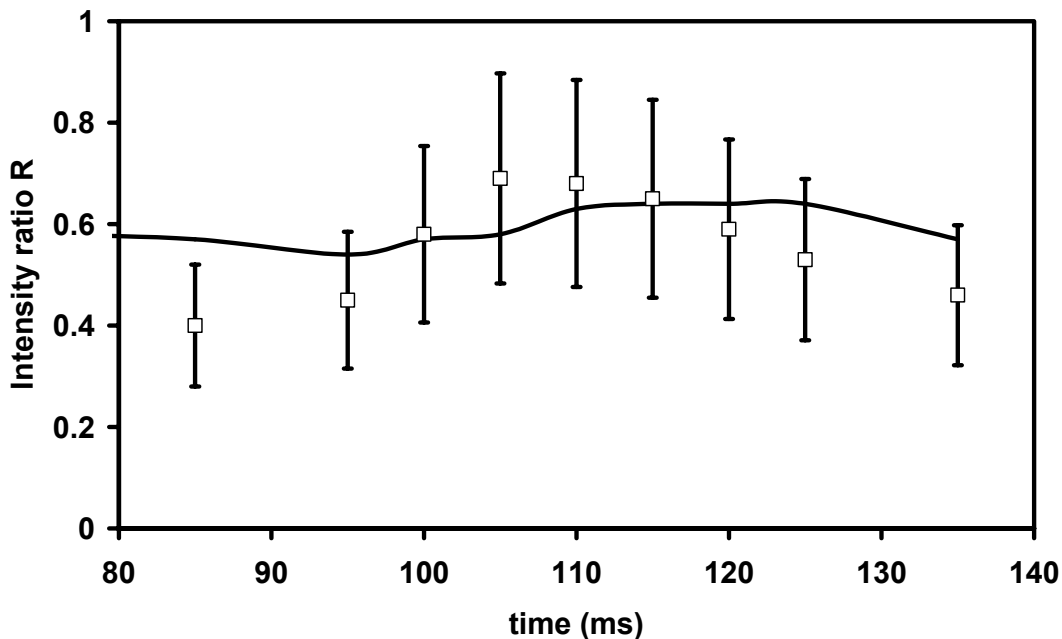


Figure 5. Intensity ratio  $R = I(2s^22p^5 \ ^2P_{3/2} - \ ^2P_{1/2})/I(2s^22p^5 \ ^2P_{3/2} - 2s2p^6 \ ^2S_{1/2})$  measured in experiments [21] (square) and calculated in paper [19] (solid line).

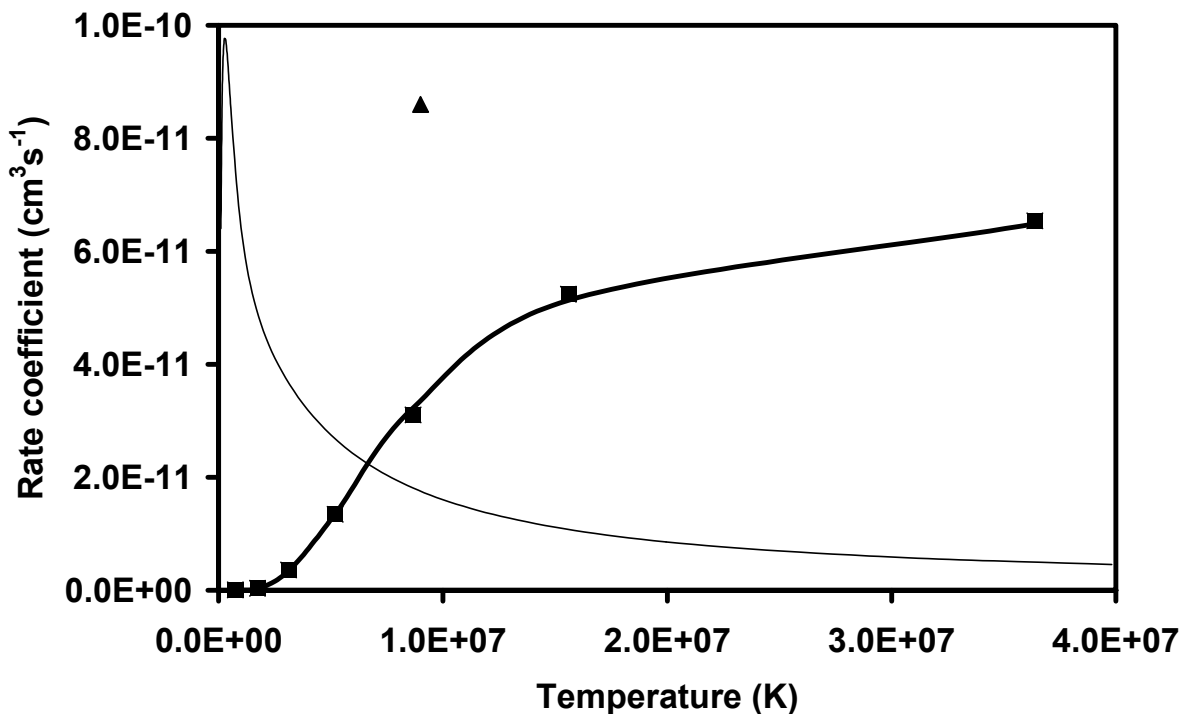


Figure 6. Collision rate coefficients for transition  $2s^22p^4 \ ^3P_2 - \ ^3P_0$  in O-like Fe XIX: solid thick lines – formula (3) for proton impact, solid thin lines – electron impact [23], ▲ – data [15], ■ - data [22].

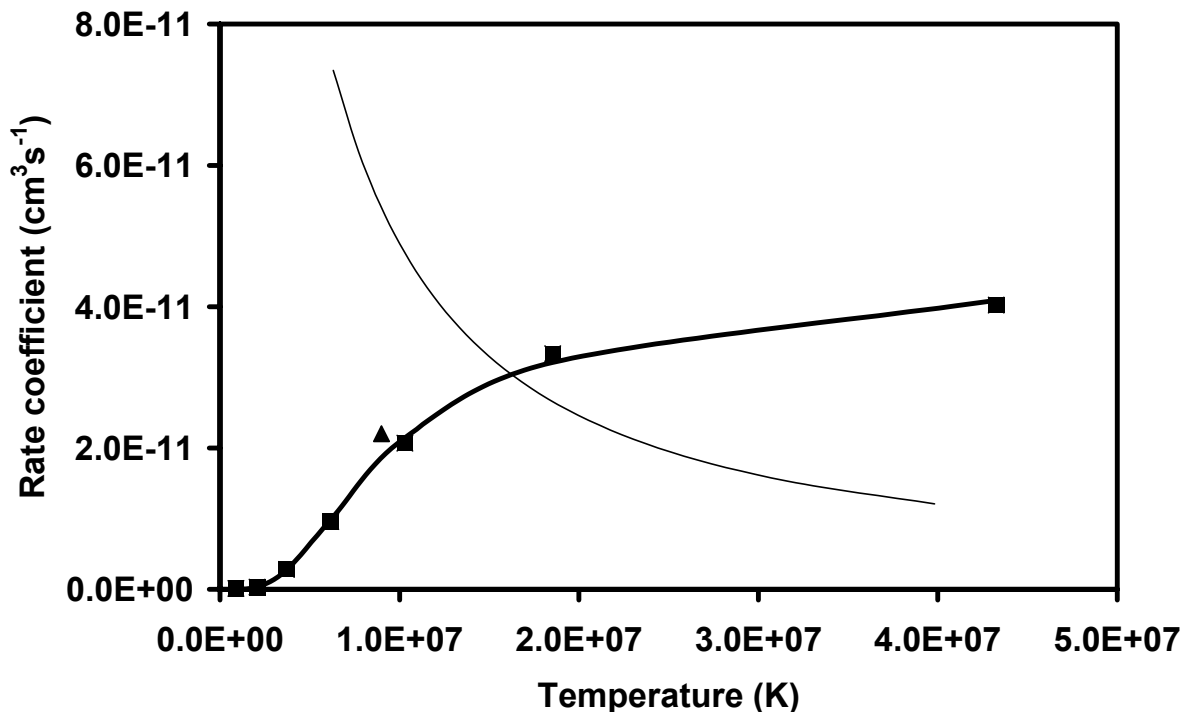


Figure 7. Collision rate coefficients for transition  $2s^2 2p^4 \ ^3P_2 - \ ^3P_1$  in O-like Fe XIX: solid thick lines – formula (3) for proton impact, solid thin lines – electron impact [23], ▲ – data [15], ■ - data [22].

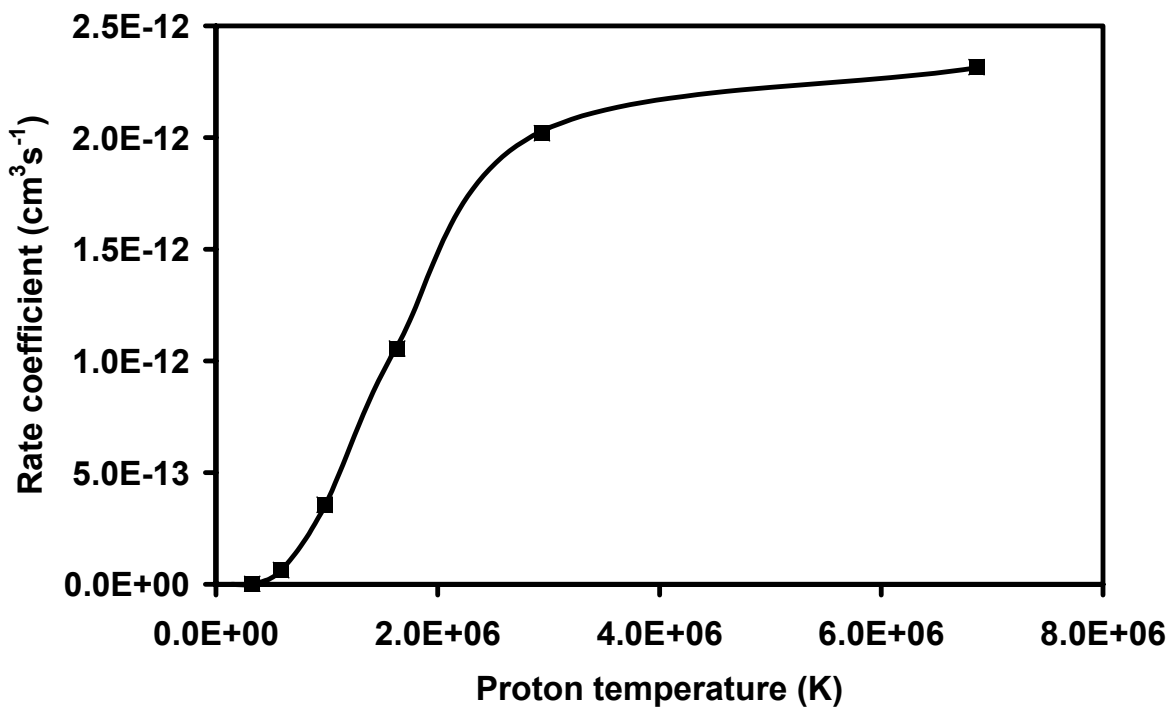


Figure 8. Collision rate coefficient for transition  $2s^2 2p^4 \ ^3P_0 - \ ^3P_1$  in O-like Fe XIX: solid thick lines – formula (3) for proton impact, ■ - data [22].

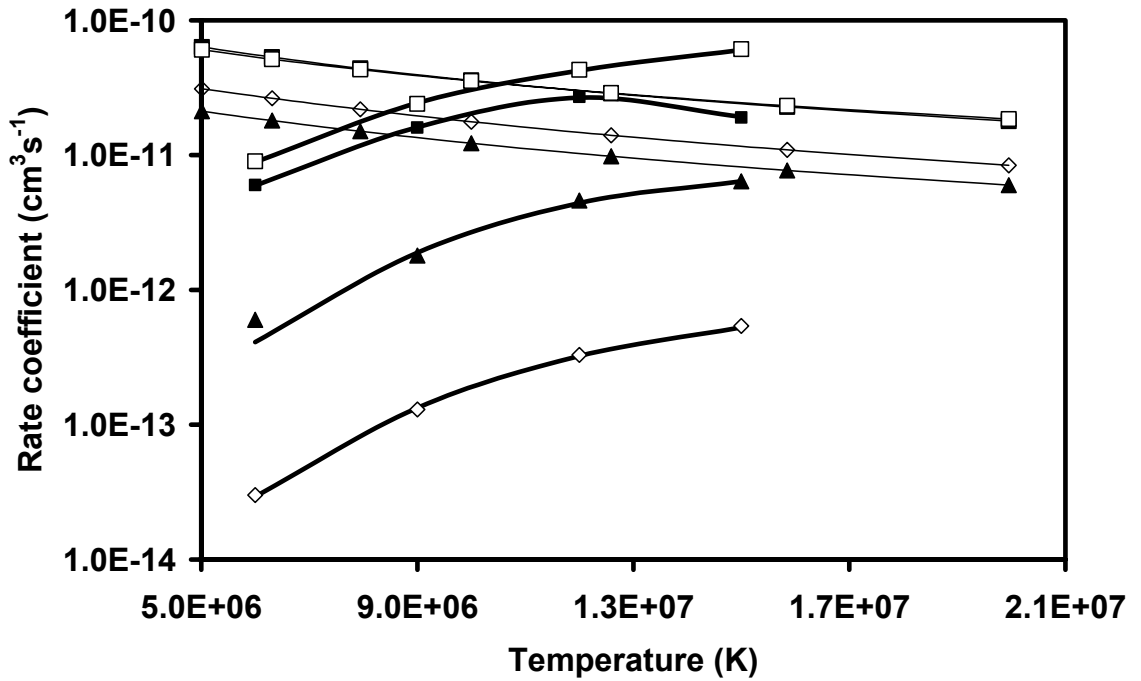


Figure 9. Collision rate coefficients for transitions  $2s^22p^3\ ^4S_{3/2} - ^2D_{3/2}$  (■),  $2s^22p^3\ ^4S_{3/2} - ^2D_{5/2}$  (□),  $2s^22p^3\ ^4S_{3/2} - ^2P_{1/2}$  (▲),  $2s^22p^3\ ^4S_{3/2} - ^2P_{3/2}$  (◇) in N-like Fe XX: solid thick lines – formula (3) for proton impact, solid thin lines – electron impact [27], ▲, ■, □, ◇ - data [25].

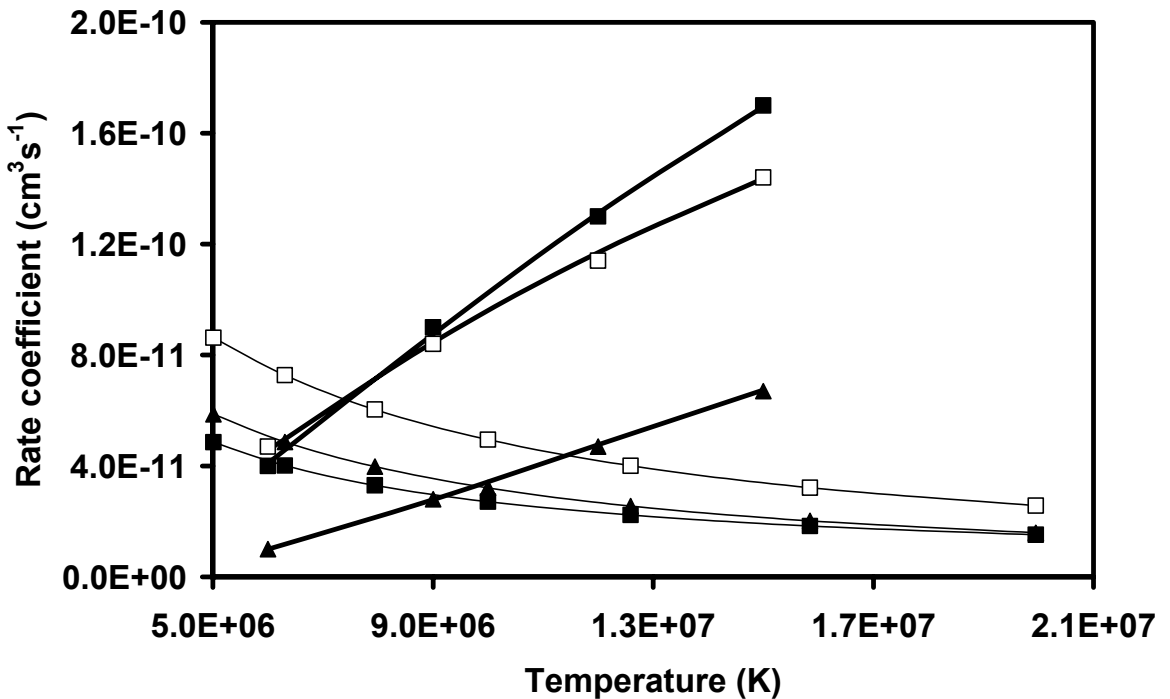


Figure 10. Collision rate coefficients for transitions  $2s^22p^3\ ^2D_{3/2} - ^2D_{5/2}$  (□),  $2s^22p^3\ ^2D_{3/2} - ^2P_{1/2}$  (■),  $2s^22p^3\ ^2D_{3/2} - ^2P_{3/2}$  (▲) in N-like Fe XX: solid thick lines – formula (3) for proton impact, solid thin lines – electron impact [27], ▲, ■, □ - data [25].

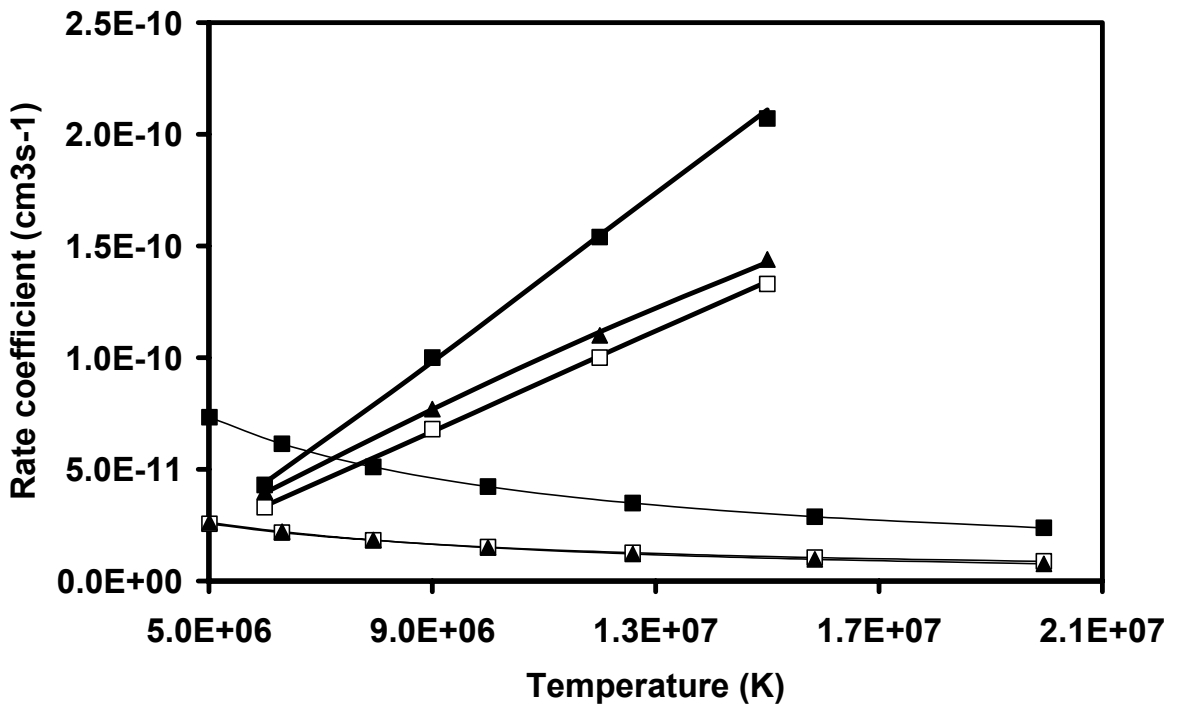


Figure 11. Collision rate coefficients for transitions  $2s^22p^3 \ ^2D_{5/2} - \ ^2P_{1/2}$  ( $\square$ ),  $2s^22p^3 \ ^2D_{5/2} - \ ^2P_{3/2}$  ( $\blacksquare$ ),  $2s^22p^3 \ ^2P_{1/2} - \ ^2P_{3/2}$  ( $\blacktriangle$ ) in N-like Fe XX: solid thick lines – formula (3) for proton impact, solid thin lines – electron impact [27],  $\blacktriangle$ ,  $\blacksquare$ ,  $\square$  - data [25].

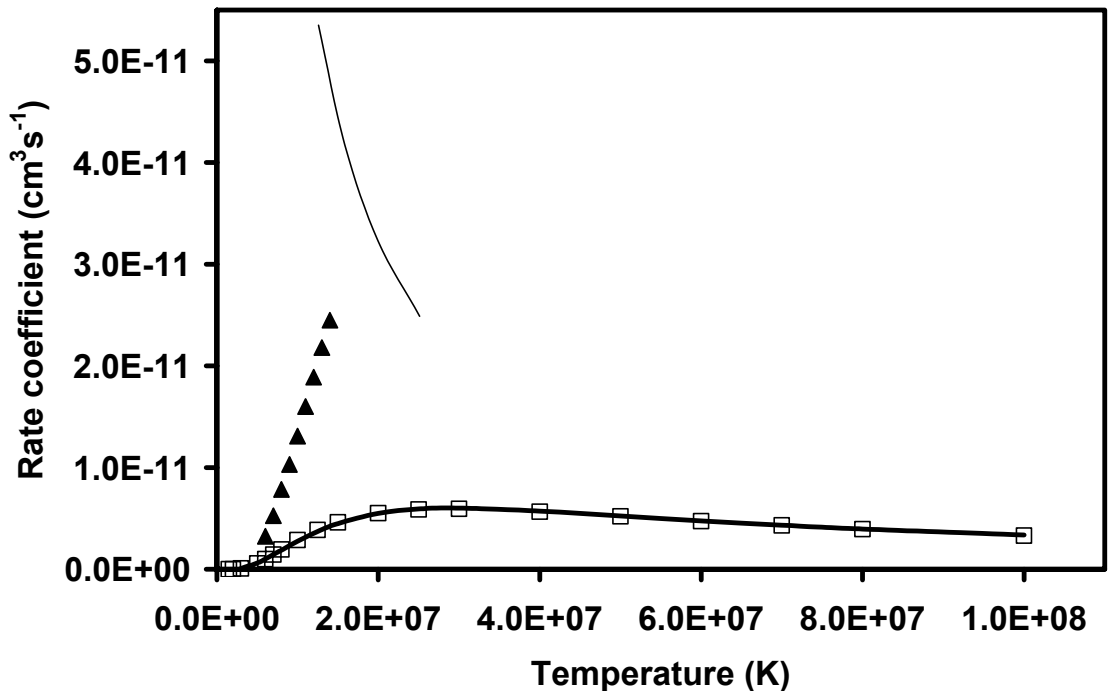


Figure 12. Collision rate coefficients for transition  $2s^22p^2 \ ^3P_0 - \ ^3P_1$  in C-like Fe XXI: solid thick line – formula (3) for proton impact, solid thin line – electron impact [31],  $\blacktriangle$  data [30],  $\square$  - data [29].

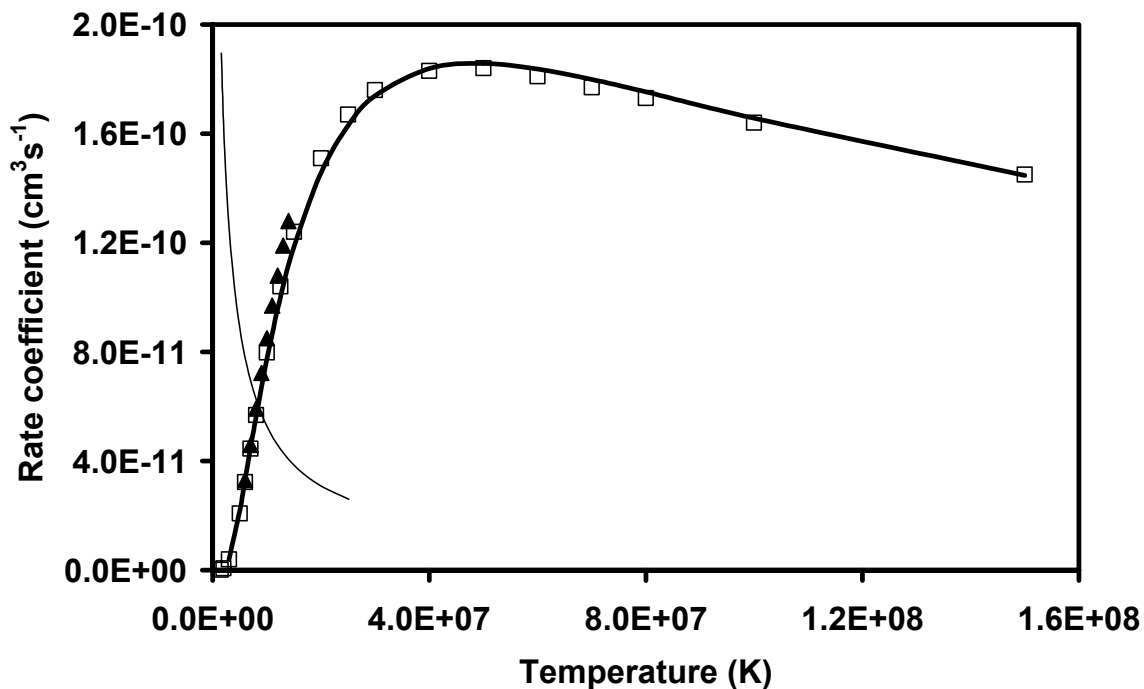


Figure 13. Collision rate coefficients for transition  $2s^2 2p^2 \ ^3P_0 - \ ^3P_2$  in C-like Fe XXI: solid thick line – formula (3) for proton impact, solid thin line – electron impact [31],  $\blacktriangle$  data [30],  $\square$  - data [29].

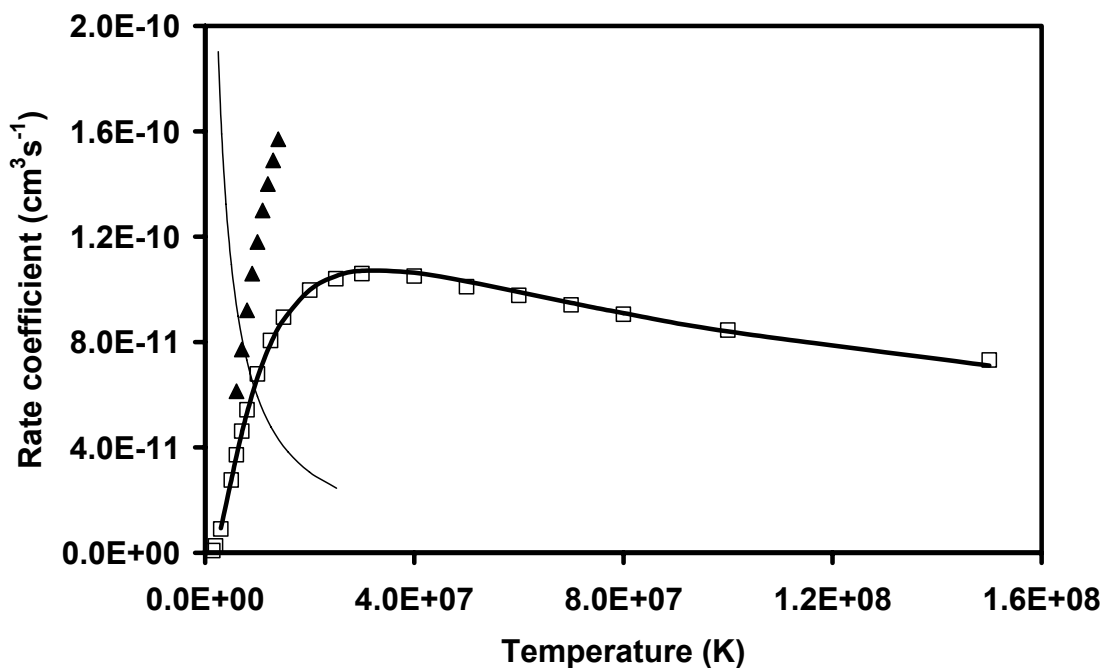


Figure 14. Collision rate coefficients for transition  $2s^2 2p^2 \ ^3P_1 - \ ^3P_2$  in C-like Fe XXI: solid thick line – formula (3) for proton impact, solid thin line – electron impact [31],  $\blacktriangle$  data [30],  $\square$  - data [29].

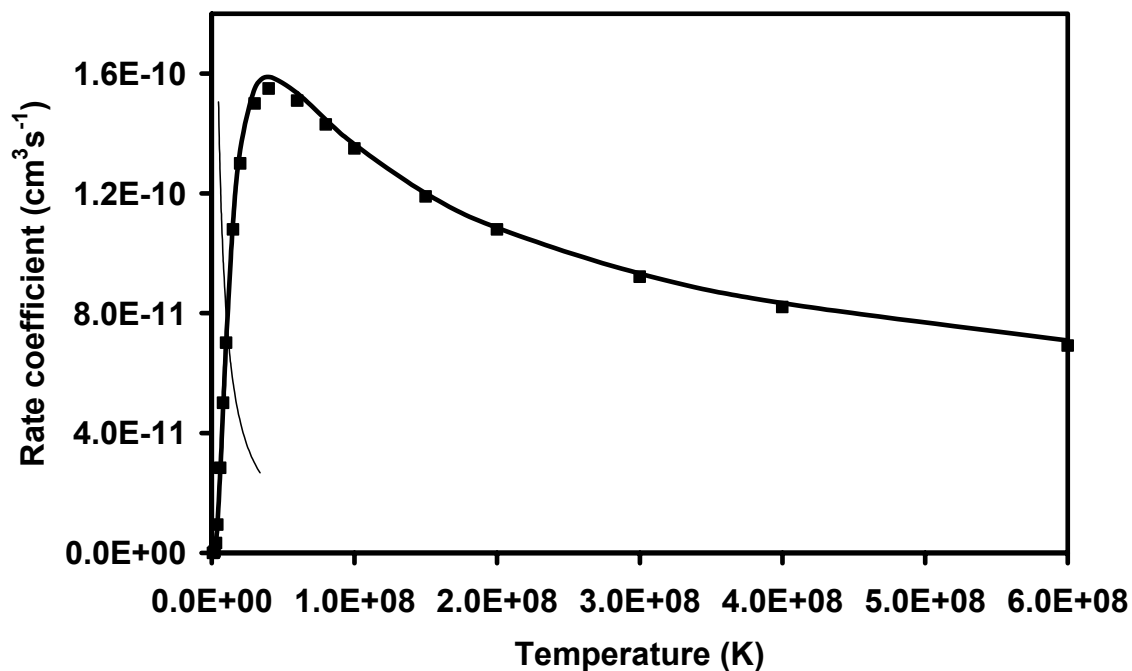


Figure 15. Collision rate coefficients for transition  $2s^2 2p \ ^2P_{1/2} - ^2P_{3/2}$  in B-like Fe XXII: solid thick line – formula (3) for proton impact, solid thin line – electron impact [35], ■ - data [34].

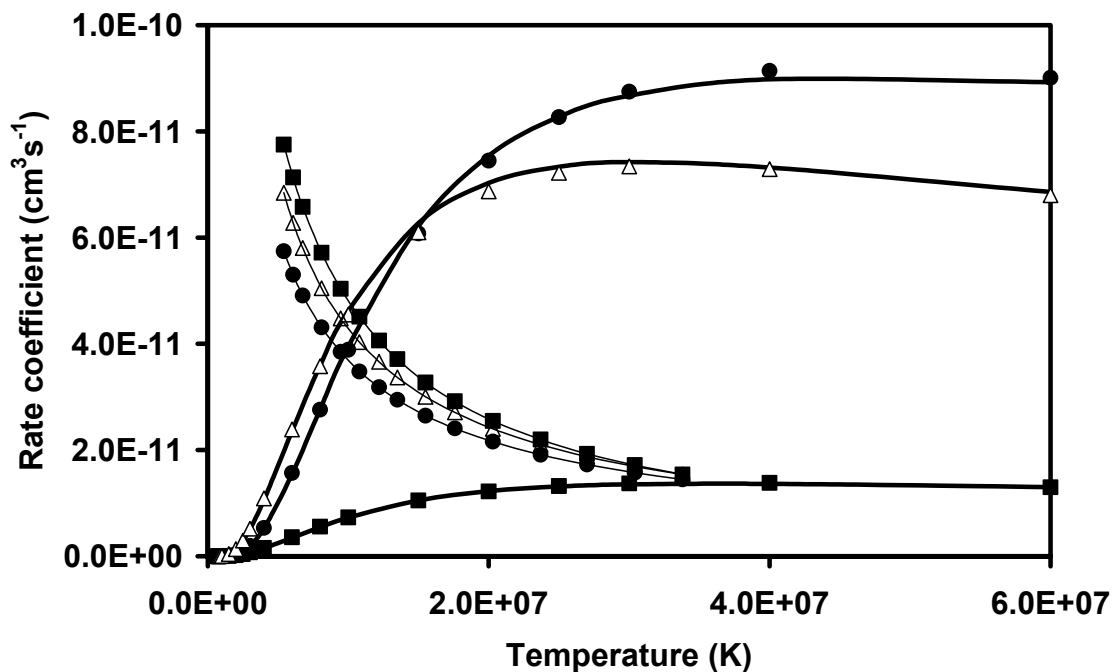


Figure 16. Collision rate coefficients for transition  $2s^2 2p^2 \ ^4P_{1/2} - ^4P_{5/2}$  (●),  $2s^2 2p^2 \ ^4P_{3/2} - ^4P_{5/2}$  (Δ),  $2s^2 2p^2 \ ^4P_{1/2} - ^4P_{3/2}$  (■), in B-like Fe XXII: solid thick line – formula (3) for proton impact, solid thin line – electron impact [35], ●, Δ, ■ - data [34].



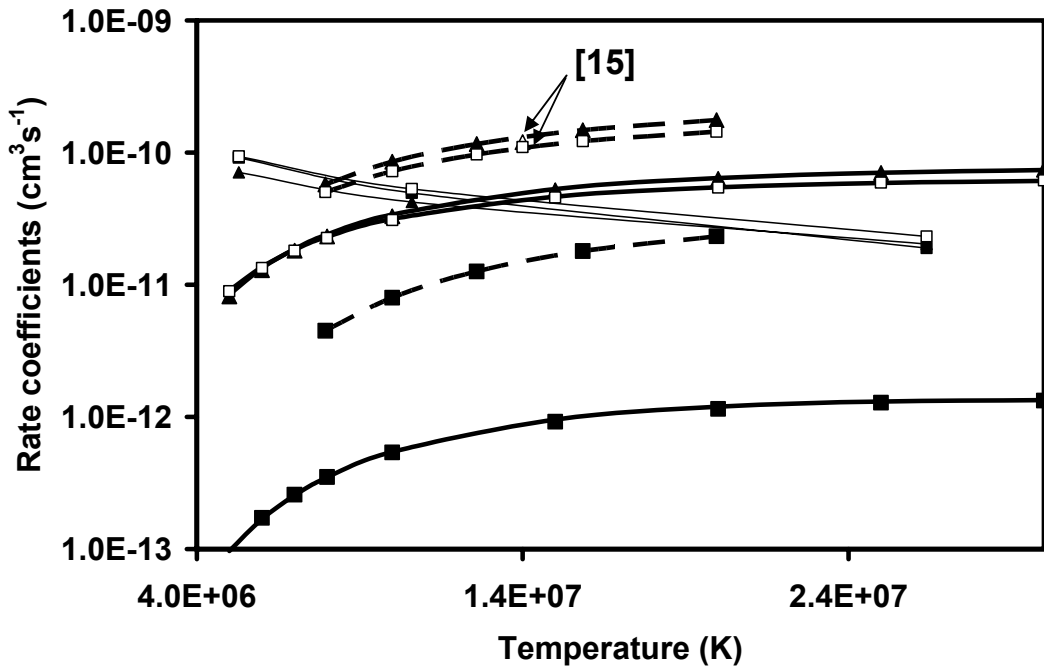


Figure 17. Collision rate coefficients for transition  $2s2p \ ^3P_0 - \ ^3P_2$  ( $\blacktriangle$ ),  $2s2p \ ^3P_1 - \ ^3P_2$  ( $\square$ ),  $2s2p \ ^3P_0 - \ ^3P_1$  ( $\blacksquare$ ) in Be-like Fe XXII [37]: solid thick line – formula (3) for proton impact, solid thin line – electron impact [38], thick dashed lines - data [36]. Two points of data [15] are only at  $T=1.4 \times 10^7$  K.